

# Solar PV Generation System with AC Terminal Voltage Control Capability

Cyrus Wekesa \*

Tokuo Ohnishi \*

## Abstract

The conventional solar PV system inverter normally operates at unity power factor and has not additional function to improve the line voltage quality. This paper investigates in detail the AC terminal voltage control of the proposed solar PV generation system with frequency tracking ability. The system is composed of two loops, one to control real power for sending the generated power and the other to control reactive power to compensate for utility voltage drops. The terminal voltage for stand-alone operation can also be controlled within the dc voltage control range. Simulation results show successful control of the system for various cases.

**Key Words:** Solar PV System, Autonomous Control, Terminal Voltage Control, Reactive Power, Frequency Tracking.

## 1. Introduction

Electric power distribution lines, especially weak rural feeder lines, experience decreasing bus voltages as the distance from the distribution transformer increases, and the voltage may become lower than the utility allows. This problem is typically mitigated by increasing the tap ratio of the distribution transformers and/or switching on shunt capacitors. However, solar photovoltaic generation systems extensively embedded within the low voltage distribution network of the utility supply may not only help level the load curve and avoid costs associated with upgrading of power transmission lines, transformers and switchgear, but can also improve the voltage profile across the feeder through generation of reactive power.

Because residential consumers are typically charged only for the active power that they draw from the utility, conventional solar PV systems are usually designed to operate at unity power factor, a design strategy which maximizes the benefits of the individual consumer [1]. However, the solar PV system inverter's real power output is typically less than the apparent power rating, meaning that solar PV systems can be operated at a power factor less than unity to generate reactive power and help control utility line voltage. Also, the solar PV system can serve as an active harmonic filter.

Some solar PV systems with reactive-power generating capability are described in the literature. Borle [2] describes a utility-interactive solar PV power conditioning system which provides voltage support through reactive power control. However, the scheme controls the magnitude and not the instantaneous terminal voltage. In our scheme, the instantaneous terminal voltage is controlled, a factor which can enable removal of harmonic waveforms so that the instantaneous terminal voltage waveform exactly matches the generated reference voltage waveform.

The proposed solar PV system extends the system by Ohnishi [3] to enable not just reactive power generation, but also active harmonic filtering. It enables easy system extension because in a network of multiple systems, each solar PV system is controlled individually as opposed to the conventional phase control method based on a common synchronous signal. Whereas in [3], the inverter output voltage ( $e_o$ ) is kept constant and equal to the generated reference value, in the proposed system described in this paper (Fig.1), the system configuration is changed to keep the load terminal voltage ( $e_r$ ) constant instead. This allows the inverter output voltage ( $e_o$ ) to vary within allowable limits. That is, the inverter's reactive power output is limited by the maximum allowable voltage at its bus, and the reactive power generation varies automatically in response to detected changes in voltage at the point of load connection, restoring the terminal voltage to the desired value. The Maximum Power Point Tracking (MPPT) control can be easily attained by adjusting the reference dc-link voltage  $E_{dr}$  for the utility interconnection mode. In the paper, we describe mainly the utility terminal voltage control.

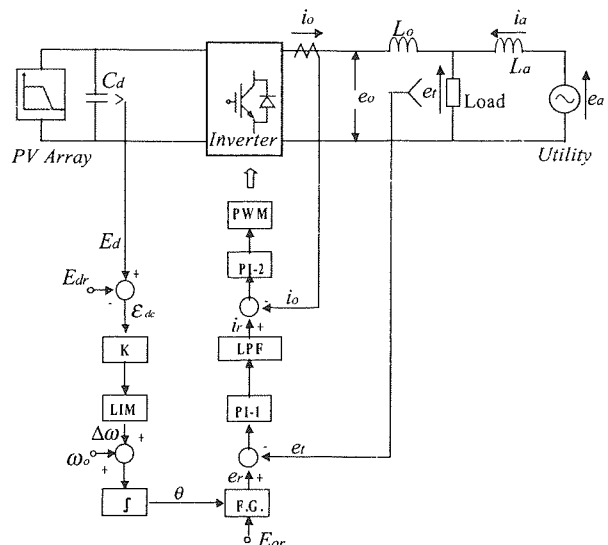


Fig. 1. Proposed solar PV system configuration.

\* Department of Electrical and Electronic Engineering, The University of Tokushima, 2-1, Minami-Josanjima, Tokushima-shi, 770-8506

(原稿受付：2003年2月24日)

## 2. The PV System Operation and Analysis

### 2.1 System Operation and Theoretical Analysis

In Fig. 1, the PV Array charges the capacitor  $C_d$  to a voltage  $E_d$ .  $E_d$  is compared with a reference voltage  $E_{dr}$  to generate an error signal which is then amplified and passed through a limiter. The output  $\Delta\omega$  is added to base frequency  $\omega_o$ , and the operating frequency  $\omega$  is given by eq. (1). This resultant frequency signal is used to generate a reference voltage signal ( $e_r$ ).

$$\omega = \omega_o + \Delta\omega \tag{1}$$

The limiter keeps the frequency of the PV system within defined limits. By this control loop, the operating frequency of the inverter can track the utility line frequency, and in stand-alone mode, the operating frequency is decided by the load [3]. The controller (PI-1) keeps the load voltage  $e_l$  at reference value  $e_r$ , and controller (PI-2) keeps inverter output current  $i_o$  at  $i_r$ , with an error signal to provide the required modulating signal. Any high frequency signals out of the voltage controller are removed by the low-pass filter (LPF). The magnitude of  $E_{or}$  in Fig. 1 is set so that  $e_r$  has a peak value of 282.84 V. To limit the dc side voltage ripple, a sufficient capacitor  $C_d$  is used. If, as in Fig. 1,  $E_d$  is the input dc voltage and  $m$  is the modulation index, then the utility voltage  $e_a$  and the inverter output voltage  $e_o$  are given by eq. (2) and eq. (3).

$$e_a = \sqrt{2}E_a \sin \omega_o t = \sqrt{2}E_a \sin \theta \tag{2}$$

$$e_o = mE_a \sin \omega t = mE_a \sin \theta \tag{3}$$

The reference current ( $i_r$ ) is composed of real and reactive components with a power factor angle ( $\varphi$ ) as given in eq. (4). This can be simplified to eq. (5) and eq. (6) for the respective real and reactive current components.

$$i_r = \sqrt{2}I_{rp} \sin \theta + \sqrt{2}I_{rq} \cos \theta \tag{4}$$

$$i_r = \sqrt{2}I_r \sin(\theta + \varphi) = i_o \tag{5}$$

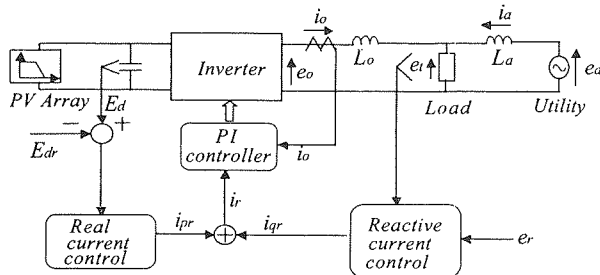


Fig. 2. Power conditioning system block diagram.

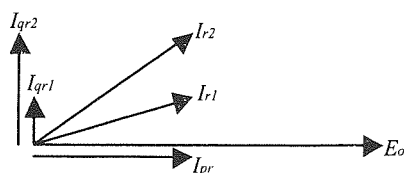


Fig. 3. Changing reactive current magnitude reference ( $I_{qr}$ ).

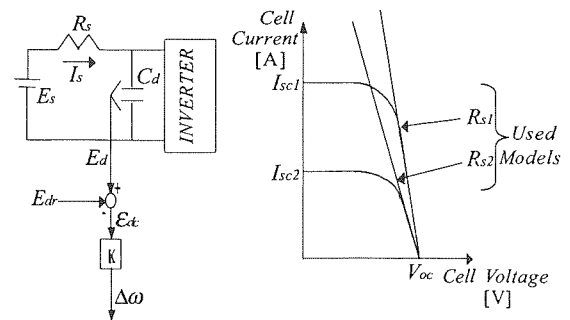


Fig. 4. Model of dc-side of the PV system.

$$i_r = i_{pr} + i_{qr} \tag{6}$$

Fig. 2 is the simplified power conditioning system control, where two loops operate to control the real and reactive power flow in the inverter. The dc-link voltage control loop provides the real current magnitude reference ( $i_{pr}$ ); a separate reactive power control loop provides the reactive current magnitude reference ( $i_{qr}$ ). For a given real current magnitude reference ( $I_{pr}$ ), the variation of the reactive current magnitude reference ( $I_{qr}$ ) is shown in Fig. 3 for two cases. When the terminal voltage ( $E_l$ ) decreases more due to heavier load on the utility, the PV system control enables a correspondingly higher reactive reference current ( $I_{qr2}$ , Fig. 3), necessary for voltage control.

Fig. 4 shows the model of the dc-side of the PV system, where the dc supply  $E_s$  and the series resistance  $R_s$  represent a model of the solar array. From eq. (1) and Fig. 4, the PV system operating frequency ( $f_{AC}$ ) is given by eq. (7) and depends on the voltage error, which in turn depends on the load experienced for stand-alone case. Based on Fig. 1 and Fig. 4, the deviation from the nominal frequency is given by eq. (8) and the array current  $I_s$  by eq. (9). The absolute maximum value of the frequency deviation from the nominal is set by the limiter to  $\Delta\omega_m$ .

$$f_{AC} = \frac{\omega_o + \Delta\omega}{2\pi} \tag{7}$$

$$\Delta\omega = K(E_s - I_s R_s - E_{dr}) \tag{8}$$

$$I_s = \frac{(\omega_o - 2\pi f_{AC}) + K(E_s - E_{dr})}{KR_s} \tag{9}$$

Assuming  $E_d$  constant, instantaneous inverter power input  $P_{in}(t)$  and output  $P_{out}(t)$  are given by eq. (10) and eq. (11), where  $E_o$  and  $I_o$  are the inverter rms output voltage and current respectively. Thus, the inverter input current  $i_{inv}(t)$  is given by eq. (12).

$$P_{in}(t) = E_d i_{inv}(t) \tag{10}$$

$$P_{out}(t) = E_o I_o \cos \varphi - E_o I_o \cos(2\omega t + \varphi) \tag{11}$$

$$i_{inv}(t) = \frac{E_o I_o}{E_d} (\cos \varphi - \cos(2\omega t + \varphi)) \tag{12}$$

This current,  $i_{inv}(t)$ , is also given by the difference between the PV array current  $I_s$  and the capacitor current  $i_c(t)$  as in eq. (13).

From eq. (12) and eq. (13), the capacitor current is then given by eq. (14).

$$i_{inv}(t) = I_s - i_c(t) \quad (13)$$

$$i_c(t) = \frac{E_o I_o \cos(2\omega t + \varphi)}{E_d} \quad (14)$$

From eq. (14), the voltage ripple across the inverter is given by eq. (15) and the maximum ripple value by eq. (16).

$$v_{c,ripple}(t) = \frac{1}{C_d} \int i_c(t) dt = \frac{1}{2\omega C_d} \frac{E_o I_o}{E_d} \sin(2\omega t + \varphi) \quad (15)$$

$$v_{c,ripple(max)} = \frac{1}{2\omega C_d} \frac{E_o I_o}{E_d} \quad (16)$$

By specifying the allowable ripple voltage, the required capacitor can be selected using eq. (16).

## 2.2 Reactive Power and PV System Inverter Rating

Shown in Fig. 5 is the interaction between the solar PV system and the utility supplying a common load. The solar system inverter output voltage at bus A has a magnitude  $E_o$ , while the load voltage at bus B has a magnitude  $E_l$ . Typically, the voltage  $E_o$  at bus A leads the voltage  $E_l$  at bus B, and the goal is to keep  $E_l$  constant.

It is known that the flow of real power ( $P$ ) between two points such as A and B in Fig. 5 depends on the phase angle between the voltages  $E_o$  and  $E_l$ , whereas the flow of reactive power ( $Q$ ) between the same points is determined by the scalar voltage difference between the two voltages. Thus, making the assumption of a completely lossless reactive link, then the load voltage  $E_l$  can be approximated by eq. (17), where  $I_{oq}$  is the reactive current component of the PV system output current ( $I_o$ ) and  $I_{lq}$  is the load reactive current component. This is in accordance with the fact that reactive power flows towards the node of lower voltage whenever a scalar voltage difference exists across a largely reactive link [4]. Thus,  $E_l$  can be maintained constant by automatically adjusting  $I_{oq}$  as appropriate in response to changes in the voltage at the connection point B. In eq. (17), the PV system is providing leading reactive current (in accordance with Fig. 2 and Fig. 3) to supply the lagging reactive power required by most loads and thus improve voltage.

$$E_l \approx E_a - X_a(I_{lq} - I_{oq}) \quad (17)$$

The active power out of the inverter ( $P$ ) is determined by the amount of power that is supplied by the PV solar array and the inverter's efficiency, and for a given active power output, the inverter's reactive power output ( $Q$ ) is limited by the inverter's nominal apparent power rating.

The inverter bus voltage  $E_o$  will vary so as to generate needed reactive power to keep load voltage  $E_l$  constant. Thus, the inverter's reactive power output will necessarily be limited by the maximum allowable bus voltage ( $E_{omax}$ ). Another limitation is the regulation imposed by the utility company regarding the power factor at which the distributed generation systems embedded within the utility should operate.

The considered system is based on a 5 kW rated inverter, de-

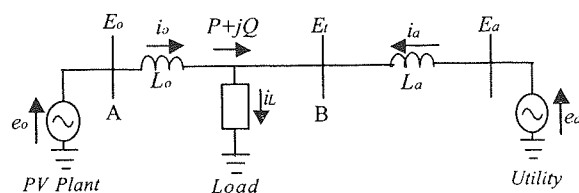


Fig. 5. PV system and utility: voltage support at B.

pending on the available solar radiation. It is also assumed that the utility imposes a minimum operating power factor of 0.85 [1]. On this basis, the apparent power rating of the inverter is estimated at 6.0 kVA while the maximum reactive power is estimated at 3.0 kVar. With the load voltage ( $E_l$ ) desired to be maintained constant at approximately 200 V, the maximum allowable inverter output voltage ( $E_{omax}$ ) is taken to be about 5% higher than the required load voltage. Thus,  $E_{omax}$  is estimated at 210 V.

## 3. System Simulation Parameters

Proper operation to allow the PV system to deliver power to the utility occurs when the dc-link capacitor voltage ( $E_d$ ) is greater than the peak utility voltage. Also, at maximum power point (MPP), the voltage of a solar cell is by design about 80% the open-circuit voltage [5]. From this, the dc reference voltage is selected to be 320 V, so that the PV system will be operating in the vicinity of the reference voltage. The value of the dc-link capacitor ( $C_d$ ) is selected to minimize the dc-side voltage ripple. In this case, the dc-side voltage ripple is limited to less than 1% of the dc-link voltage, based on eq.(16). For a system rated at 5 kW, the PV output current ( $I_o$ ) in eq.(16) is estimated at 25 A, and the inductor  $L_o$  is chosen so as to limit switching frequency harmonics. With a switching frequency of 15 kHz, and on the basis of the explained considerations and the use of PSIM Software, the capacitor  $C_d$  and other system parameters are summarized in Table 1 and Table 2.

Table 1. External simulation parameters.

Parameter (Symbol)	Value
PV Array [5 kW]	400 [V] DC Supply $R_{s1} = 5\Omega$ $R_{s2} = 10\Omega$
$C_d$	10000 [uF]
$L_o, L_a$	0.2, 0.5 [mH]
$E_d$	320 [V]
Base Frequency $\omega_o$	377 [rad/sec]
Inverter Voltage, Frequency	200 [V], 60 [Hz]
Utility Voltage, Frequency	200 [V], 60 [Hz]

Table 2. Controller, limiter and filter parameters.

Parameter	Value
PI-1 Time Constant	0.5 [sec]
PI-1 Gain	100
PI-2 Time Constant	0.5 [sec]
PI-2 Gain	0.3
Integrator() Time Constant	1.0 [sec]
K	1.0
Low-Pass Cut-off	60 [Hz]
Low-Pass Damping Ratio	0.7
Filters Gain	1.0
Limiter $\Delta\omega_u$	$\pm 5.0$ [rad/sec]

### 4. Simulation Results

Some results obtained from simulations as well as through theoretical analyses for some cases are shown in Fig. 6 to Fig. 13. Fig. 6 shows the special case for stand-alone operation mode at 60.33 Hz frequency. The frequency in this case depends on the load as shown in Fig. 7. The waveforms for the various utility-interactive operation cases are shown in Fig. 8 to Fig. 10. Fig. 8 shows rated PV system capacity and utility at 60.0 Hz, Fig. 9 shows rated PV system capacity and utility at 60.5 Hz and Fig. 10 shows half the rated PV system and utility at 60.0 Hz. Fig. 11 shows the power balance when both the PV system and the utility are connected in parallel, supplying an increasing load. Fig. 12 shows the voltage levels for three cases: the utility alone, the utility working with a unity power factor PV system and the utility working with the proposed system in this paper. Finally, Fig. 13 shows the variation of the generated reactive power with loading for both the simulated and analytical cases.

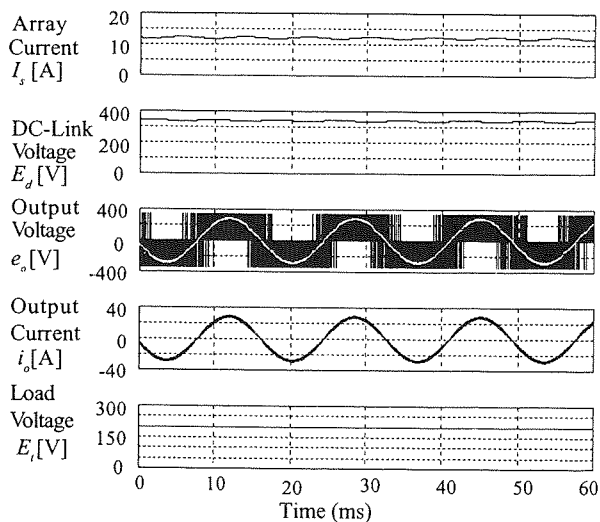


Fig. 6. PV system operation: stand-alone case at 60.33 Hz.

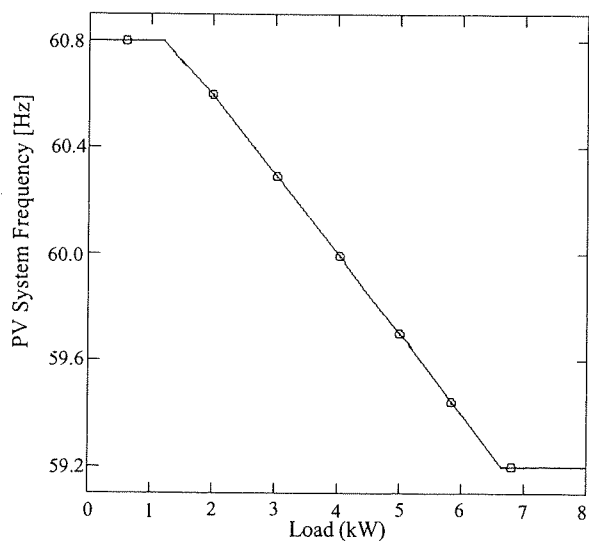


Fig. 7. PV system frequency with loading: stand-alone.

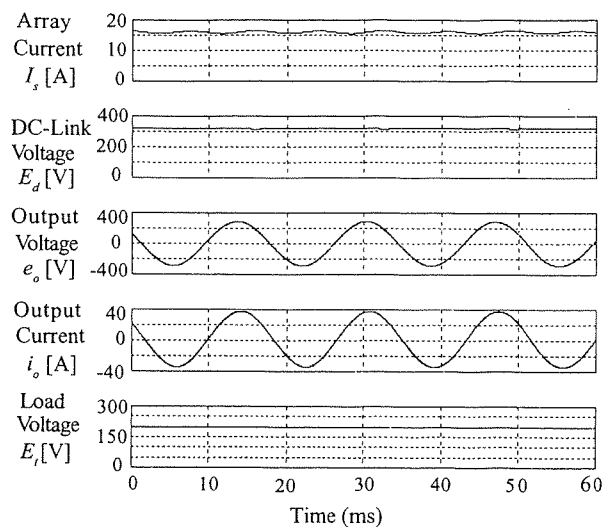


Fig. 8. PV system and utility at 60.0 Hz: rated capacity.

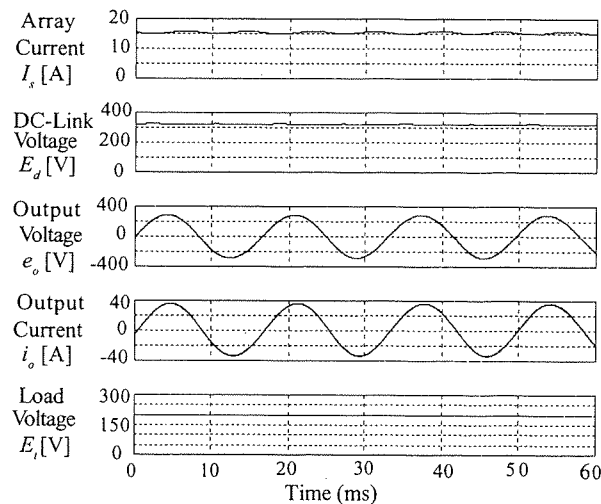


Fig. 9. PV system and utility at 60.5 Hz: rated capacity.

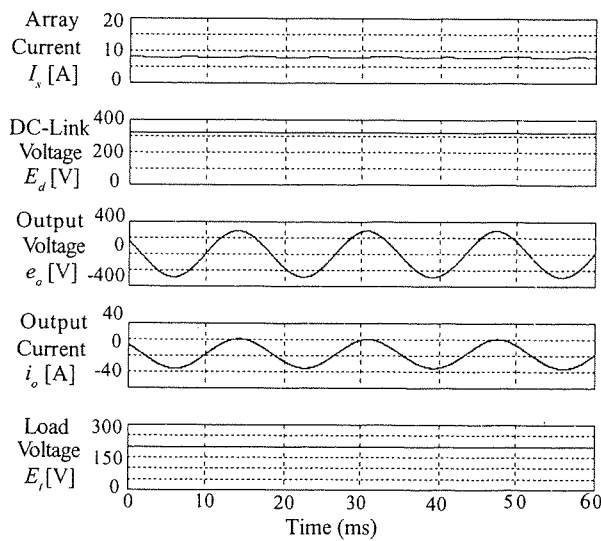


Fig. 10. PV system and utility at 60.0 Hz: half capacity.

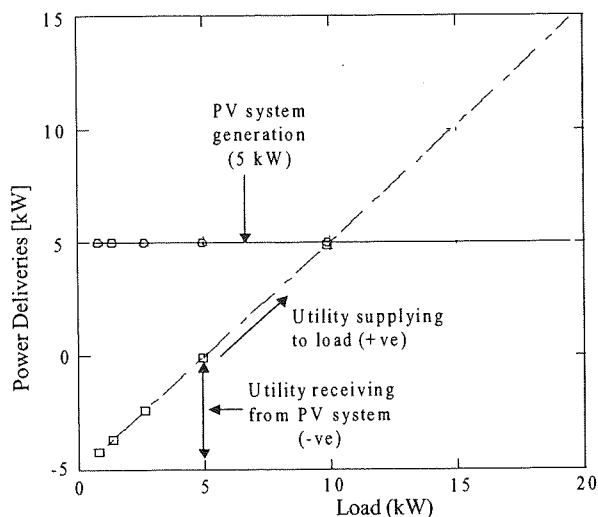


Fig. 11. PV system and grid power vs. load demand (60 Hz).

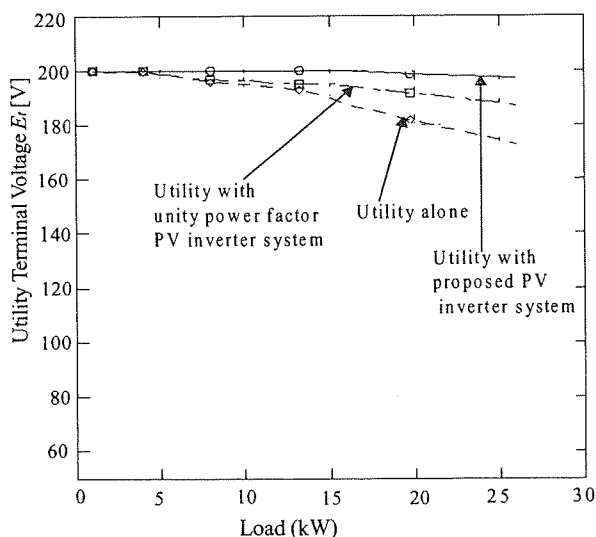


Fig. 12. Voltage control for different cases (5 kW system).

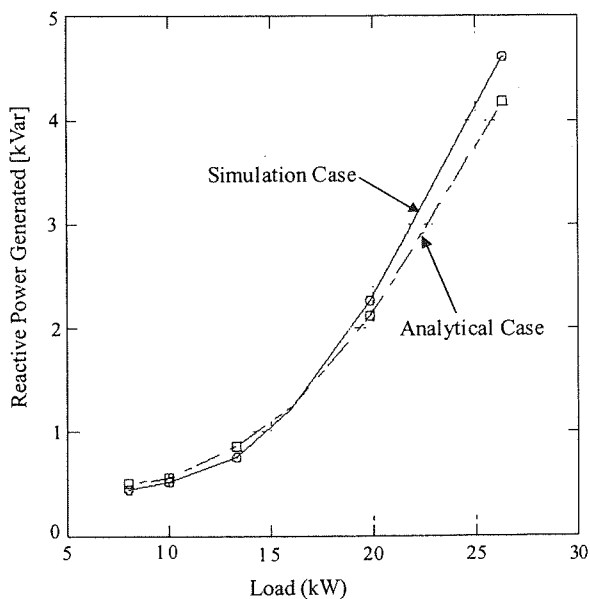


Fig. 13. PV system reactive power as load increases.

## 5. Discussion of Results

### 5.1 Stand-alone Consideration

Although Fig. 6 shows a case for the PV system in stand-alone operation mode at 60.33 Hz, the system operating frequency is generally determined by the load placed on the system, as seen from Fig. 7 and eq. (9). This is because the charging level of the dc-link capacitor ( $C_d$ ) will vary in response to changing load. With limiter setting values restricting frequency operation within defined limits, it follows that with a nominal frequency of 60.0 Hz, the PV system frequency will be bound within the 59.2 Hz - 60.8 Hz range.

From eq. (9) describing the relationship between the array current ( $I_s$ ) and the PV system frequency ( $f_{ac}$ ), re-arranging eq. (9) results into eq. (18), and substituting the parameters for the values in Table 1 and Table 2 gives the frequency expression in eq. (19).

$$f_{ac} = \frac{\omega_o - K(E_{dr} - E_s)}{2\pi} - \frac{K}{2\pi} I_s R_s \quad (18)$$

$$f_{ac} = 72.73 - \frac{I_s R_s}{2\pi} \quad (19)$$

Then using the frequency limits set by the limiter and substituting in eq. (19) gives eq. (20) as the voltage drop across  $R_s$  in Fig. 4. Then with the dc supply at 400 V, the voltage range across the dc-link capacitor is given by eq. (21).

$$75 \leq I_s R_s \leq 85 \quad (20)$$

$$315 \leq E_d \leq 325 \quad (21)$$

Thus, working in stand-alone mode, the PV system should operate within these limits in order to fulfil the frequency requirements. These conditions mean that the loading to which the PV system is subjected to has to be within the limits which will lead to a final system operating frequency within the acceptable limits as determined by the limiter settings. The above equations are verified by simulation results shown in Fig. 7.

### 5.2 Utility-Interactive Mode and Voltage Support

In utility interactive operation mode, the PV system frequency tracks the utility frequency through slight adjustments in the dc-link voltage in accordance with eq. (7) and eq. (8). However, the same conditions discussed above for stand-alone mode still apply so that for proper PV system operation within the set frequency bounds, eq. (21) has to be satisfied. Thus, while the PV system frequency tracks the utility frequency, this only happens when the utility frequency falls within 59.2 Hz - 60.8 Hz.

Fig. 8 to Fig. 10 demonstrate operation in utility-interactive mode. At 60 Hz utility frequency (Fig. 8), the PV system operates well just as it does at 60.5 Hz (Fig. 9). This is due to changes in the voltage across the capacitor, enabling the system to automatically adjust to the utility frequency while delivering the same amount of power as determined by the rating of the system. At half the PV system capacity (Fig. 10), the array

current is halved but the dc-link capacitor voltage stays within the range of the reference voltage.

In Fig. 11, showing the PV system and utility power as loading increases (for 60.0 Hz utility frequency), when the demand is less than the supply from the PV system, the excess power is delivered to the utility; this is shown as negative power (received by the utility). When the demand exceeds the PV system generation, the extra demand is supplied from the utility; this is shown as positive power (drawn from the utility). The active power output from the PV system is determined by the amount of power that is supplied by the solar array, as well as the efficiency of the inverter.

The utility terminal voltage control feature of the PV system is illustrated in Fig. 12, showing the utility without a solar PV system, utility with a unity power factor PV system and the utility with the proposed PV system. The three cases demonstrate the capability of the proposed system to improve voltage much better than can be achieved by a conventional, unity power factor PV system. The effect of voltage compensation is more pronounced at higher loads as Fig. 12 shows. The described system is rated at 5 kW and for load demand greater than this, the extra demand is supplied from the utility. Thus, above a loading of 5 kW, the usefulness of the PV system in terms of voltage compensation through reactive power generation becomes more evident. For comparison purposes, at a load of 26 kW, the percentage voltage drop is 13.5% with the utility operating alone, but changes to 1.5% with the use of the described PV system.

In Fig. 13, the variation of reactive power generated by the PV system to control the voltage at the PV system connection point as loading increases is shown, both from an analytical viewpoint as well as from the actual simulations obtained. In the analytical case, the assumption is made for constant terminal voltage ( $E_t$ ) at 200 V; in practice, with heavy loading on the system, the PV system is unable to deliver the required reactive power because of its rating limits. Thus, at high loads, the simulation result shows higher reactive power demand because the terminal voltage ( $E_t$ ) is decreasing as shown previously in Fig. 12. From both cases, reactive power generation increases as the loading on the utility increases.

## 6. Concluding Remarks

The operation of the solar PV system with terminal voltage control capability has been described, from which it is observed through analysis and simulation results that the PV system delivers not only active power to the load and any excess power to the utility, but also delivers reactive power at the point of connection, helping control the utility line voltage at the PV system connection point. The system is able to operate well both at the nominal frequency of the utility and when the utility frequency changes slightly within certain specific limits. In utility interactive mode, the PV system operating frequency is determined by the utility frequency, and the control of the system enables it to adjust accordingly to changes in utility frequency. In stand-alone mode, the solar PV system frequency continuously changes within a narrow range in response to loading. It is considered that widespread use of distributed genera-

tion systems like the PV system with frequency tracking ability described in this paper, based on control of real and reactive power flows in the inverter, will improve the voltage profile of the utility supply in the distribution network.

## References

- (1). M. Begovic, A. Pregelj, A. Rohatgi, D. Novosel, *Impact of Renewable Distributed Generation on Power Systems*, Proc. of the 34th Hawaii International Conference on System Sciences, 2001.
- (2). L. J. Borle, M. S. Dymond, V.V. Nayar, *Development and Testing of a 20 kW Grid-Interactive Power Conditioning System in Western Australia*, IEEE Transactions on Industry Applications, Vol. 33, No. 2, March/April 1997, pp502-508.
- (3). T. Ohnishi, M. Furuhashi, K. Kawasaki, *Solar Power Generation System Installed Individually for Local Power Network System*, Transactions of IEE Japan, Vol. 115-D, No.12, Dec. 1995, p1448-1455.
- (4). B.M. Weedy, *Electric Power Systems*, Second Edition, John Wiley & Sons, 1972, pp 42-46.
- (5). C.V Nayar, S.M Islam, and H. Sharma, *Power Electronics for Renewable Energy Sources*, Power Electronics Handbook, Academy Press, 2001, pp540-541.